FACULTY OF SCIENCE AND TECHNOLOGY

MASTER THESIS

Study programme / specialisation:

Mathematics and physics
Specialisation physics

The spring semester, 20.22.

Open / Confidential

Author: Aslak Matre

Aslak Matre
.....
(signature author)

Course coordinator: Alex Bentley Nielsen

Supervisor(s): Alexander Karl Rothkopf

Thesis title:

Real time simulation of quarkonium in a thermal medium using a 3D Lindblad equation

Credits (ECTS): 60

Keywords:
Quarkonium
Real time simulation
Lindblad equation
Open quantum system

Pages: 29

+ appendix: 0

Stavanger, 15/06/2022
date/year

Real time simulation of quarkonium in a thermal medium using a 3D Lindblad equation

Aslak Matre

15.06.2022

Abstract

Using a new finite difference operator RN-SBP that has recently been developed and used for 1D simulations of the Lindblad equation, we extend it to the 3D case. We have not quite been able to implement the RN-SBP properly for 3D, but we have proved that it will preserve the trace if implemented correctly. We have also showed that the coherent dynamics of the Lindblad equation in 3D, and the recoiless limit in 3D works as intended.

Contents

1 Introduction

We humans have always been a curious kind. All since we first appeared on the east African plateau some 300 thousand years ago, we have been trying to figure out how the world we live in works. It may have been simple at first, possibly smashing rocks together to see what it is made up. But as we humans grew more and more technologically advanced, our methods of finding out how the universe works have grown more sophisticated as well. But it is not only technology that has grown, but also our understanding, and model of how and what the universe is made up of and works. Our history can trace its origin all they way back to pre-Socratic Greece, with the philosopher Democritus, with his atomic theory of the universe. But it is in the last 150 years or so, that our understanding of the microscopic world has really accelerated. From Einsteins nobel winning treaty of Brownian motion, the discovery of the electron by J. J. Thomson, Rutherfords discovery of the nucleus of the atom, our current model of the subatomic world, the Standard Model has a proud lineage to look back on. But our understanding isn't complete, and may never be. Currently, to find out what is beyond the Standard Model, we are crashing protons and protons, and heavy ions together at the LHC. In these collisions, briefly, the conditions inside will be extreme, to the point where ordinary matter break down to its constituent components, into a new state of matter, which we call quark gluon plasma. This state of matter has been theorized to have filled the early universe before it cooled down. So understanding the behavior of this state of matter isn't just useful in understanding of quantum chromodynamics, but also in our quest of understanding the origin and the early universe.

But then how can we understand the behavior of the quark gluon plasma? How can measure the conditions inside the quark gluon plasma? Since the time duration of these collision are so shor, on the order of femtoseconds, there is no chance that we can put any sort of external probe into the quark gluon plasma, let it thermalize, and then measure the properties of the probe. But what we can do, is to use collision byproducts, that can thermalize inside the collision center, and then measure the properties of that particle to reconstruct the collision center. And we have just such a candidate that is a good match for the job we are looking for. And that particle is heavy quarkonium.

Then the question we want to answer becomes, how can we use quarkonium particle to get information about the collision? To answer that question, we will turn to the framework of open quantum systems. We will be treating the quarkonium as a distinguishable particle from medium, and then evolve the particle forwards, to get an understanding of how the medium impacts the evolution of the particle.

In the first section of the thesis, we will go into some background knowledge that might be useful before going forward. In the next section, we will be talking about the influence functional from Feynman and Vernon. In the third section, we will be talking about the Lindblad equation, that we will use to simulate the system. The next section will be about numerics, such as the new RN-SBP finite difference operator. Next section we will be discussing the results we got from our simulations. And finally in the last section, we will be wrapping things up with the conclusion and outlook towards the future.

Throughout this thesis we will working in natural units, that is $c = \hbar = m_e = \varepsilon_0 = 1$, unless explicitly stated otherwise. Other units will be derived from this. Most things will be measured in electron volts, eV, such as mass, energy, temperature, and more.

1.1 Short intro QCD

For our introduction to quantum chromodynamics, shorthanded to QCD, let us start with QCD Lagrangian, for one particle

$$\mathcal{L}_{QCD} = \bar{\psi}_i \left(i\gamma^\mu (D_\mu)_{ij} - m\delta_{ij} \right) \psi_j - \frac{1}{4} G^a_{\mu\nu} G^{\mu\nu}_a \tag{1.1}$$

where $G^a_{\mu\nu}$ is the gluon field strength tensor

$$G^a_{\mu\nu} = \partial_\mu A^a_\mu - \partial_\nu A^a_\nu + g f^{abc} A^b_\mu A^c_\nu \tag{1.2}$$

described by the potential A^a_μ. g is the strong coupling constant, which decides the strength of the QCD interaction, f^{abc} are the structure constants. ψ is the quark field. The covariant derivative D_μ for QCD is

$$D_\mu = \partial_\mu - igG^a_\mu t^a, \tag{1.3}$$

where G^a_μ is gluon gauge tensor(?) and $t^a = \frac{\lambda^a}{2}$, where λ^a is the Gell-Mann matrices which are representations of the $SU(3)$ group, in which QCD are built upon. The indices written in the Latin script, such as a in t^a are color indices, and takes values from 1 to 8.

One curious fact is that of asymptotic freedom in QCD. In short, it says that interactions become weaker the shorter the distance is. This contrast starkly towards both electromagnetism and gravity, where interactions become stronger the shorter the distance is. Due to this, quarks inside the proton, for example, can act almost like a free particle, while it can never escape from it.

One simple model describing the confinement, is that of a Cornell potential

$$v(r) = -\frac{\alpha}{r} + \sigma r + c \tag{1.4}$$

At short distances the Coulombic part of the potential, $-\frac{\alpha}{r}$, will dominate. This part describes the gluon exchange between the quark and its anti-quark. The second linear part describes the confinement of the quark, as the interaction becomes larger and larger the further away two quarks move from each other.

What we are interested in, quarkonium. A type of heavy meson, there are two types of quarkonia, charmonium $c\bar{c}$ and bottomonium, $b\bar{b}$. So, why are we interested in using quarkonium as a probe? The biggest reason, is that it has a very clean decay channel, mainly decaying dileptons.

There have been several approaches to try to describe quarkonium in medium, for a comprehensive review, see [14]. We will only summarize things here. Some have tried to work with non-linear stochastic Schrödinger equations, one of them being the Schrödinger-Langevin equation, or SLE[7]. This equation is a Langevin like extension to the regular Schrödinger equation,

$$i\hbar \frac{\partial}{\partial t}\psi = [H_0 + \hbar A(S(x,t) - \int \psi^* S(x,t)\psi dx) - xF_R(t)]\psi \tag{1.5}$$

where $H_0$is the Hamiltonian for the subsystem, A is a friction coefficient, S is the real phase of the wavefunction ψ, and F_R is the fluctuation operator.

Another approach would be that of the rate equation[4]

$$\frac{dN_\gamma(\tau)}{d\tau} = -\Gamma_\gamma(T)[N_\gamma - N^{eq}_\gamma(T)] \tag{1.6}$$

1.2 The density matrix

The density matrix ρ was introduced in 1927 by John von Neumann[13]. It allows for descriptions of mixed ensambles of states. Therefore it contains, in addition to the quantum uncertainty, also a statistical uncertainty. The density matrix operator $\hat{\rho}$ can be defined as an other outer product of a statevector if we have a pure state

$$\hat{\rho} = |\psi\rangle \langle\psi| , \tag{1.7}$$

where $|\psi\rangle^\dagger = \langle\psi|$ or, if we have a mixed state

$$\hat{\rho} = \sum_i p_i |\psi_i\rangle \langle\psi_i| . \tag{1.8}$$

This is the density matrix operator. To get the density matrix, in a certain basis, one can write it

$$\rho = \langle e_i| \hat{\rho} |e_j\rangle , \tag{1.9}$$

or

$$\rho = \langle e_i|\psi\rangle \langle\psi|e_j\rangle \tag{1.10}$$

for an orthonormal basis e. If one has a initial density matrix $\rho(0)$ at time $t = 0$, one can evolve it using the time evolution operators U and $U^\dagger$,

$$\rho(t) = U\rho(0)U^\dagger \tag{1.11}$$

where $U(t,0) = \tau e^{-i\int H(t)dt}$, or in the case where the Hamiltionian H is time independent, $U(t) = e^{-\frac{iHt}{\hbar}}$. One can then show that the equation of motion for the density matrix will be the von Neumann equation

$$\frac{d}{dt}\rho = -i[H, \rho]. \tag{1.12}$$

For the density matrix to have physical meaning, there are three important properties it must satisfy. These three properties are: positivity of the density matrix,

$$\langle\psi| \rho |\psi\rangle > 0, \tag{1.13}$$

hermiticity

$$\rho^\dagger = \rho, \tag{1.14}$$

and unit trace, if it describes a pure state

$$Tr[\rho] = 1, \tag{1.15}$$

other wise, if it is a mixed state

$$Tr[\rho] < 1 \tag{1.16}$$

One more property that the density matrix fulfills if it is pure, is that it is idempotent

$$\rho^2 = \rho. \tag{1.17}$$

Finally, observables can be found by tracing the density matrix with an hermitian operator $\hat{A}$

$$\left\langle \hat{A} \right\rangle = Tr[\hat{\rho}\hat{A}]. \tag{1.18}$$

1.3 Path integrals

One approach towards quantum mechanics and quantum field theory, contrasting the canonical approach,

$$\langle\Omega|\, T\{\phi(x_1)...\phi(x_n)\}\,|\Omega\rangle = \frac{\langle 0|\, T\{\phi(x_1)...\phi(x_n)e^{i\int d^4x\mathcal{L}_{int}[\phi_0]}\}\,|0\rangle}{\langle 0|\, T\{e^{i\int d^4x\mathcal{L}_{int}[\phi_0]}\}\,|0\rangle} \tag{1.19}$$

is that of Richard Feynman's path integral formulation. Let us have a look at the quantum mechanical version of the path integral. Suppose we have a standard non-relativistic Hamiltonian

$$\hat{H} = \frac{\hat{p}^2}{2m} + v(x). \tag{1.20}$$

To evolve it from state $|x_i\rangle$ to a final state $\langle x_f|$, assuming the Hamiltonian is not time dependent,

$$\langle x_f|x_i\rangle = \langle x_f|\, e^{-i(t_f-t_i)\hat{H}}\,|x_i\rangle\,. \tag{1.21}$$

If the Hamiltonian is time dependent, smoothly, we can solve for an infinitesimal time step, from some step n to $n+1$

$$\langle x_{n+1}|x_n\rangle = \langle x_{n+1}|\, e^{-i\hat{H}\delta t}\,|x_n\rangle\,. \tag{1.22}$$

Expanding this, we can solve for $\langle x_f|x_i\rangle$

$$\langle x_f|x_i\rangle = \int dx_n...dx_1\,\langle x_f|\, e^{-i\hat{H}(t_f)\delta t}\,|x_{f-1}\rangle\,...\,\langle x_{i+1}|\, e^{-i\hat{H}(t_i)\delta t}\,|x_i\rangle \tag{1.23}$$

Inserting a complete set of momentum eigenstate $|p\rangle\,\langle p|$ into the infinitesimal time step above, and the non relativistic Hamiltonian,

$$\langle x_{n+1}|x_n\rangle = \int \frac{dp}{2\pi}\,\langle x_{n+1}|\,|p\rangle\,\langle p|\, e^{-i(\frac{\hat{p}^2}{2m}+v(x))\delta t}\,|x_n\rangle \tag{1.24}$$

Solving this integral we obtain

$$\langle x_{n+1}|x_n\rangle = Ne^{-iv(x)\delta t}e^{i\frac{m}{2}\delta t\frac{(x_{n+1}-x_n)^2}{\delta t}} \tag{1.25}$$

where N is normalization constant, we will just ignore. Recognizing there is a hidden Lagrangian in the exponential, we obtain

$$\langle x_{n+1}|x_n\rangle = Ne^{-iL\delta t} \tag{1.26}$$

We can then insert this into the previous equation, and taking the limit of δt to zero, we get

$$\langle f|i\rangle = N\int \mathcal{D}x(t)e^{iS[x]} \tag{1.27}$$

This is the quantum mechanical version of the path integral. For a more in depth version of the path integral, and the quantum field theory version, see Schwartz ch. 14[15].

2 Open quantum systems

2.1 Influence functional model

Feynman and Vernon's[5] influence functional model is one of the the defining models for open quantum systems. Starting with the abstract density matrix ρ. Writing it down in coordinate space, the density matrix will then take the form

$$\langle x\boldsymbol{R}|\,\rho(t)\,|y\boldsymbol{Q}\rangle = \int dx'dy'd\boldsymbol{R}'d\boldsymbol{Q}' \\ \langle x\boldsymbol{R}|\,e^{\frac{-iHt}{\hbar}}\,|x'\boldsymbol{R}'\rangle\,\langle x'\boldsymbol{R}'|\,\rho(0)\,|y'\boldsymbol{Q}'\rangle\,\langle y\boldsymbol{Q}|\,e^{\frac{iHt}{\hbar}}\,|y'\boldsymbol{Q}'\rangle\,. \quad (2.1)$$

We recognize the two terms $\langle x\boldsymbol{R}|\,e^{-\frac{iHt}{\hbar}}\,|x'\boldsymbol{R}'\rangle$ and $\langle y'\boldsymbol{Q}'|\,e^{\frac{iHt}{\hbar}}\,|y\boldsymbol{Q}\rangle$ to be the path integral over the paths x and $\boldsymbol{R}$ for

$$\langle x\boldsymbol{R}|\,e^{-\frac{iHt}{\hbar}}\,|x'\boldsymbol{R}'\rangle = \int\int \mathcal{D}x\mathcal{D}\boldsymbol{R}e^{\frac{i}{\hbar}S[x,\boldsymbol{R}]}, \quad (2.2)$$

and over y and $\boldsymbol{Q}$ for

$$\langle y\boldsymbol{Q}|\,e^{\frac{iHt}{\hbar}}\,|y'\boldsymbol{Q}'\rangle = \int\int \mathcal{D}y\mathcal{D}\boldsymbol{Q}e^{-\frac{i}{\hbar}S[y,\boldsymbol{Q}]}. \quad (2.3)$$

For shorthand notation we will call

$$\int\int \mathcal{D}x\mathcal{D}\boldsymbol{R}e^{\frac{i}{\hbar}S[x,\boldsymbol{R}]} = K(x,\boldsymbol{R},t;x',\boldsymbol{R}',0), \quad (2.4)$$

and

$$\int\int \mathcal{D}y\mathcal{D}\boldsymbol{Q}e^{-\frac{i}{\hbar}S[y,\boldsymbol{Q}]} = K^*(y,\boldsymbol{Q},t;y',\boldsymbol{Q}',0), \quad (2.5)$$

where S is the action. Similar to what we did for the Hamiltonian, we assume that the action can be written as

$$S_{tot} = S_P + S_E + S_{int}. \quad (2.6)$$

The density matrix will then take the form of

$$\langle x\boldsymbol{R}|\,\rho(t)\,|y\boldsymbol{Q}\rangle = \int dx'dy'd\boldsymbol{R}'d\boldsymbol{Q}' \\ K(x,\boldsymbol{R},t;x',\boldsymbol{R}',0)K^*(y,\boldsymbol{Q},t;y',\boldsymbol{Q}',0)\,\langle x'\boldsymbol{R}'|\,\rho(0)\,|y'\boldsymbol{Q}'\rangle \quad (2.7)$$

The density matrix still contains all the information about the medium. This is not something we are interested in right now. We will introduce what is called the reduced density matrix $\tilde{\rho}$, which we will obtain by tracing out the environment of the full density matrix, such that

$$\tilde{\rho} = Tr_E[\rho]. \quad (2.8)$$

In coordinate space, the reduced density matrix will have the form

$$\tilde{\rho}(x,y,t) = \int d\boldsymbol{R}\,\langle x\boldsymbol{R}|\,\rho(t)\,|y\boldsymbol{R}\rangle = \int dx'dy'd\boldsymbol{R}'d\boldsymbol{Q}'d\boldsymbol{R}KK^*\,\langle x'\boldsymbol{R}'|\,\rho(0)\,|y'\boldsymbol{Q}'\rangle \quad (2.9)$$

We will also suppose we can write the initial density matrix $\rho(0)$ in the the following form:

$$\rho(0) = \rho_P(0)\rho_E(0) \quad (2.10)$$

If we then plug this initial density matrix back into the definition of the reduced density matrix, we will obtain

$$\tilde{\rho}(x,y,t) = \int d\boldsymbol{R} \langle x\boldsymbol{R}| \rho(t) |y\boldsymbol{R}\rangle = \int dx'dy'd\boldsymbol{R}'d\boldsymbol{Q}'d\boldsymbol{R}KK^* \langle x'\boldsymbol{R}'| \rho_P(0)\rho_E(0) |y'\boldsymbol{Q}'\rangle \tag{2.11}$$

which can be written in terms of the propagator J

$$\tilde{\rho}(x,y,t) = \int dx'dy'J(x,y,t;x',y',0)\rho_P(x',y',0) \tag{2.12}$$

where

$$J(x,y,t;x',y',0) = \int\int \mathcal{D}x\mathcal{D}y e^{\frac{i}{\hbar}[S_P(x)-S_P(y)]}\mathscr{F}(x,y), \tag{2.13}$$

where

$$\mathscr{F}(x,y) = \int dx'dy'd\boldsymbol{R}'d\boldsymbol{Q}'d\boldsymbol{R}\rho_E(\boldsymbol{R}',\boldsymbol{Q}',0) \int\int \mathcal{D}\boldsymbol{R}\mathcal{D}\boldsymbol{Q} e^{\frac{i}{\hbar}(S_{int}[x,\boldsymbol{R}]-S_{int}[y,\boldsymbol{Q}]+S_E[\boldsymbol{R}]-S_E[\boldsymbol{Q}])} \tag{2.14}$$

is the so called influence functional. The influence functional encodes the information about the interaction between the particle, and the environment.

2.2 Caldeira Legget model

We will now be looking at specific model of the influence functional, namely the Caldeira-Legget model[3]. Suppose we have a system or an environment, for example a hot thermal bath, and a massive particle submersed in that system. Also suppose we can write the Hamiltonian for that system in the form

$$H_{tot} = H_P + H_E + H_{int}, \tag{2.15}$$

where H_{Tot} is the total Hamiltonian for the combined system, H_P is the Hamiltonian for the Hamiltonian for the massive particle, H_E is the Hamiltonian for the environment, and H_{Int} is the Hamiltonian for the interaction between the environment and the particle. We will then take H_E to have the form

$$H_P = -\frac{\hbar^2}{2M}\frac{\partial^2}{\partial x^2} + v_P(x), \tag{2.16}$$

where M is the mass of the particle, and $v(x)$ is some potential. For the Hamiltonian of the environment, we will take it to have the form

$$H_E = -\frac{\hbar^2}{2m}\frac{\partial^2}{\partial \boldsymbol{R}^2} + \frac{1}{2}\sum_{i\neq j} v_E(R_i,R_j), \tag{2.17}$$

where the environment is made up of N particles, with a mass m. $\boldsymbol{R}$ is a vector, made up of N components, $(R_1,...,R_N)$, and $v_E(R_i,R_j)$ is the potential between the $i'th$ and $j'th$ particle in the environment. Finally, the Hamiltonian for the environment-particle interaction will have the form

$$H_{int} = \sum_i v_i(x,R_i). \tag{2.18}$$

$v_i(x, R_i)$ is the potential between the massive particle, and the $i'th$ particle of the environment. The full Hamiltonian of the system will then be

$$H_{tot} = -\frac{\hbar^2}{2M}\frac{\partial^2}{\partial x^2} + v_P(x) - \frac{\hbar^2}{2m}\frac{\partial^2}{\partial \boldsymbol{R}^2} + \frac{1}{2}\sum_{i\neq j} v_E(R_i, R_j) + \sum_i v_i(x, R_i). \tag{2.19}$$

If we assume that particle is only weakly interacting with the medium, in the way that the system and the environment only interact linearly, and the environment can be described as a collection of n harmonic oscillators

$$H_{tot} = \frac{p^2}{2M} + v(x) + x\sum_n C_n R_n + \sum_n \frac{p_n^2}{2m} + \sum_n \frac{1}{2} m\omega_n^2 R_n^2 \tag{2.20}$$

where ω_n is the frequencies of the harmonic oscillators in the environment, and C_n are the coupling constants between the environment and the particle. This setup has been solved in [5], and it can be showed that the influence functional for this setup will be, if we assume the environment is in thermal equilibrium at some temperature T

$$\mathscr{F}(x, y) = e^{-\frac{1}{\hbar}\int_0^t \int_0^\tau [x(\tau)-y(\tau)][\alpha(\tau-s)x(s)-\alpha^*(\tau-s)y(s)]d\tau ds} \tag{2.21}$$

where

$$\alpha(\tau - s) = \sum_n \frac{C_n^2}{2m\omega_n}[e^{-i\omega_n(\tau-s)} + \frac{e^{i\omega_n(\tau-s)}}{e^{\frac{\hbar\omega_n}{kT}} - |} + \frac{e^{-i\omega_n(\tau-s)}}{e^{\frac{\hbar\omega_n}{kT}} - |}] \tag{2.22}$$

where k is the Boltzmann constant. Since the system is in thermal equilibrium, the initial density matrix for the environment can be written as

$$\rho_E(\boldsymbol{R}', \boldsymbol{Q}', 0) = \prod_n \rho_E^k(R_n', Q_n', 0) \tag{2.23}$$

where

$$\rho_E^k(R_n', Q_n', 0) = \frac{m\omega_n}{2\pi\hbar sinh(\frac{\hbar\omega_n}{kT})} e^{-\{\frac{m\omega_n}{2\hbar sinh(\frac{\hbar\omega_n}{kT})}[R_n'^2 + Q_n'^2 cosh(\frac{\hbar\omega_n}{kT}) - 2R_n'Q_n']} \tag{2.24}$$

Writing the α in terms of real and imaginary components

$$\alpha_R(\tau - s) = \sum_n \frac{C_n^2}{2m\omega_n} coth(\frac{\hbar\omega_n}{2kT}) cos(\omega_n[\tau - s]) \tag{2.25}$$

$$\alpha_I(\tau - s) = -\sum_n \frac{C_n^2}{2m\omega_n} sin(\omega_n[\tau - s]) \tag{2.26}$$

Writing down the propagator J for this gives us

$$\begin{aligned} J(x, t, t; x', y', 0) = \int\int \mathcal{D}x\mathcal{D}y e^{\frac{i}{\hbar}[S_P(x) - S_P(y)]} \\ e^{-\frac{1}{\hbar}\int_0^t \int_0^\tau [x(\tau)-y(\tau)][\alpha_I(\tau-s)[x(s)+y(s)]d\tau d} \\ e^{-\frac{1}{\hbar}\int_0^t \int_0^\tau [x(\tau)-y(\tau)][\alpha_R(\tau-s)[x(s)-y(s)]d\tau d} \end{aligned} \tag{2.27}$$

This model describes quantum Brownian motion of a point particle, though it is not completely obvious how it does it.

In the classical limit, it will turn into the Fokker Planck equations.

3 Lindblad equation

So, why can't we use the Caldeira-Legget model? There are some shortcomings of that model that we would like to address. The two main reasons being that it treats the particle in the medium as a point particle, which, as a non elementary particle, it is not. Also, the Caldeira-Legget model does also not take color rotations of the quarkonium into consideration. The approach, however, that we would like to take, is that of the Lindblad master equation. The Lindblad, or Gorini–Kossakowski–Sudarshan–Lindblad(GSKL) equation, derived independently by Lindblad[9] and Gorini, Kossakowski and Sudarshan[6], both in 1976. We start with the same setup we had before, with a environment, and a massive particle submersed into that environment. As one can imagine, the central object in question becomes the density matrix ρ. Again, the density matrix will describe the entire system, which we are not interested in this case. We will therefore trace out the environment, such that we get the reduced density matrix $\tilde{\rho}$. We then want to find time evolution of said reduced density matrix. So, how can we find the time evolution for the reduced density matrix. The time evolution of it is implemented in what is called a dynamical map $V(t)$, such that

$$\tilde{\rho}(t) = V(t)\tilde{\rho}. \tag{3.1}$$

What this dynamical map is, depends on the system, but can be in general highly complicated and non trivial. But if we employ a markovian approximation of the system, IE. if the next time step of the system has no memory effect, that it only depends how the system is at this current step, and not on any other previous steps, we can reduce the complexity of $V(t)$, to the form $V(t_1 + t_2) = V(t_1)V(t_2)$. Then the question becomes, when is the markovian approximation applicable? The markovian approximation will, for our system in question, be applicable when there is separation of time scales, between of the relaxation scale of the particle τ_{re}, and the fast damping of correlations in environment τ_E, IE. we have

$$\tau_E \ll \tau_{re}. \tag{3.2}$$

Fast damping of correlations in environment τ_E tells us about the timescale in which correlations we have in the environment decays.

From this one, and using the born approximation, which says that the system is weakly coupled witht the environment, will arrive at a linear evolution equation for $\tilde{\rho}$,

$$\frac{d}{dt}\tilde{\rho} = \mathcal{L}\tilde{\rho}, \tag{3.3}$$

where $\mathcal{L}$is a generator for the dynamical map $V(t)$

$$V(t) = e^{\mathcal{L}t}. \tag{3.4}$$

As shown in [9, 6], the Lindblad equation will have this form:

$$\frac{d}{dt}\tilde{\rho} = Tr_M[\rho, H]$$

$$\frac{d}{dt}\tilde{\rho} = -i[\tilde{H_P}, \tilde{\rho}] + \sum_k \gamma_k(\hat{L}_k\tilde{\rho}\hat{L}_k^\dagger - \frac{1}{2}\hat{L}_k^\dagger\hat{L}_k\tilde{\rho} - \frac{1}{2}\tilde{\rho}\hat{L}_k^\dagger\hat{L}_k) \tag{3.5}$$

Looking very much like a modified von Neumann equation, the first part is just that, and governs the coherent evolution of the density matrix. The real meat in this equation comes in the second part, where γ_k is the damping rates, and $\hat{L}$ are the so called Lindblad operators. For a more proper derivation of this equation, see[11].

3.1 Lindblad Operators

The Lindblad operators are a manifestation of the influence functional $\mathscr{F}$, as they are the ones that carry the information about how the particle interacts with environment.

So, what is the Lindblad operators for our system. It has been shown that[1, 12], if we assume that the energy density of the system is high enough, that is larger than Λ_{QCD}, but still smaller than the mass of the quark, such that it is the largest energy scale of the system,

$$m_Q \gg T \gg \Lambda_{QCD} \tag{3.6}$$

the Lindblad operator will have the form of

$$\hat{L}_{k,a} = \sqrt{\frac{\tilde{D}(k)}{2L^3}}[e^{\frac{ik\cdot\hat{x}_Q}{2}}(1-\frac{k\cdot\hat{p}_Q}{4MT})e^{\frac{ik\cdot\hat{x}_Q}{2}}(t^a\otimes 1) - e^{\frac{ik\cdot\hat{x}_{\bar{Q}}}{2}}(1-\frac{k\cdot\hat{p}_{\bar{Q}}}{4MT})e^{\frac{ik\cdot\hat{x}_{\bar{Q}}}{2}}(1\otimes t^{a*}), \tag{3.7}$$

and the Hamiltonian will have the form

$$\tilde{H}_P = \frac{\hat{p}_Q^2+\hat{p}_{\bar{Q}}^2}{2M} + [\hat{v}(\hat{x}_Q-\hat{x}_{\bar{Q}}) - \frac{1}{8MT}\{\hat{p}_Q-\hat{p}_{\bar{Q}}, \nabla D(\hat{x}_Q-\hat{x}_{\bar{Q}})\}] \tag{3.8}$$

What does each term inside of Lindblad operators do? First up, is $\sqrt{\frac{\tilde{D}(k)}{2L^3}}$. This is the dissipative kernel, in Fourier space. What does the next part does? We see that there are two terms, with each term corresponding to the quark and the anti-quark that makes up the quarkonium particle. Inside each if the terms, there are two parts. $\frac{k\cdot\hat{p}_Q}{4MT}$describes the recoil that the quarkonium particle feel experience in the medium, when it collides with the particles in the medium, and takes care of the dissipation of energy of the quarkonium. $e^{\frac{ik\cdot\hat{x}_Q}{2}}t^a\otimes 1$ relates to the color shifts that the quarkonium can undergo, that is, it will rotate the color that the quarkonium have. It will also shift the momentum it have by $\vec{k}$[12]. The recoiless limit, which we will see more to later, is achieved by setting the parenthesis in the Lindblad operators to 1, such that we are left with

$$\hat{L}_{k,a} = \sqrt{\frac{\tilde{D}(k)}{2L^3}} \tag{3.9}$$

With a change of reference frame to the center of mass frame, and introducing relative coordinates $\hat{x}$ and $\hat{y}$, instead of the quark and anti-quark coordinates

$$\hat{x} = \frac{\hat{x}_Q+\hat{x}_{\bar{Q}}}{2}, \tag{3.10}$$

$$\hat{y} = \hat{x}_Q - \hat{x}_{\bar{Q}}, \tag{3.11}$$

$$\hat{P} = \hat{p}_Q + \hat{p}_{\bar{Q}}, \tag{3.12}$$

$$\hat{p} = \frac{\hat{p}_Q-\hat{p}_{\bar{Q}}}{2} \tag{3.13}$$

we can rewrite the Lindblad operator into the following form:

$$\hat{L}^{rel}_{k,a} = \sqrt{\frac{\tilde{D}(k)}{2L^3}}[1-\frac{k}{4MT}\cdot(\frac{1}{2}\hat{P}+\hat{p})]e^{\frac{ikr}{2}}(t^a\otimes 1) - \sqrt{\frac{\tilde{D}(k)}{2L^3}}[1-\frac{k}{4MT}\cdot(\frac{1}{2}\hat{P}-\hat{p})]e^{-\frac{ikr}{2}}(1\otimes t^{a*}). \tag{3.14}$$

It was shown in [8, 12]that the dissipative kernel of the static pair of quark anti-quark pair would be

$$D(\vec{r}) = g^2T\int\frac{d^3k}{(2\pi)^3}\frac{\pi m_D^2 e^{i\vec{k}\cdot\vec{r}}}{k(k^2+m_D^2)^2} \tag{3.15}$$

3.2 Lindblad equation for quarkonium

Evaluating the Lindblad equation in position space, it will stay linear with respect to the density matrix, but it will have spatial and temporal varying coefficients. [10] showed that when we do evaluate it in position space, it becomes

$$\begin{aligned}\frac{\partial}{\partial t}\rho(x,y,t) = i[\frac{\nabla_x^2}{M} + v(\vec{x})] - i[\frac{\nabla_y^2}{M} + v(\vec{y})]\rho(\vec{x},\vec{y},t) \\ + [2F_1(\frac{\vec{x}-\vec{y}}{2}) - 2F_1(\vec{0}) + F_1(\vec{x}) + F_1(\vec{y}) - 2F_1(\frac{\vec{x}+\vec{y}}{2})]\rho(\vec{x},\vec{y},t) \\ - [\frac{(\nabla_x^2)^2 A(\vec{x})}{4M^2} + \frac{(\nabla_y^2)^2 A(\vec{y})}{4M^2}]\rho(\vec{x},\vec{y},t) \\ + [2F_2(\frac{\vec{x}-\vec{y}}{2}) + 2F_2(\vec{x}) - 2F_2(\frac{\vec{x}+\vec{y}}{2}) - \nabla_x\frac{(\nabla_x^2)A(\vec{x})}{M^2}]\nabla_x\rho(\vec{x},\vec{y},t) \\ + [-2F_2(\frac{\vec{x}-\vec{y}}{2}) + 2F_2(\vec{y}) - 2F_2(\frac{\vec{x}+\vec{y}}{2}) - \nabla_y\frac{(\nabla_y^2)A(\vec{y})}{M^2}]\nabla_y\rho(\vec{x},\vec{y},t) \\ + [2F_3^{ij}(\frac{\vec{x}-\vec{y}}{2}) + 2F_3^{ij}(\frac{\vec{x}+\vec{y}}{2})]\frac{\partial}{\partial x_i}\frac{\partial}{\partial y_j}\rho(\vec{x},\vec{y},t) \\ + [\frac{1}{3}F_3^{kk}(\vec{0})\delta^{ij} + F_3^{ij}(\vec{x})]\frac{\partial}{\partial x_i}\frac{\partial}{\partial x_j}\rho(\vec{x},\vec{y},t) \\ + [\frac{1}{3}F_3^{kk}(\vec{0})\delta^{ij} + F_3^{ij}(\vec{y})]\frac{\partial}{\partial y_i}\frac{\partial}{\partial y_j}\rho(\vec{x},\vec{y},t) \quad (3.16)\end{aligned}$$

where we have summarized most of the $D(\vec{x})$ into 3 different F terms. Here, $A(\vec{x}) = \frac{D(\vec{x})}{8T^2}$. They read

$$F_1(\vec{x}) = D(\vec{x}) + \nabla_x^2\frac{D(\vec{x})}{4MT} + \frac{(\nabla_x^2)^2 A(\vec{x})}{8M^2} \quad (3.17)$$

$$F_2(\vec{x}) = \vec{\nabla}_x(\frac{D(\vec{x})}{4M} + \frac{\nabla_x^2 A(\vec{x})}{4M^2}) \quad (3.18)$$

$$F_3^{ij}(\vec{x}) = -\frac{\partial}{\partial x_i}\frac{\partial}{\partial x_j}\frac{A(\vec{x})}{4M^2} \quad (3.19)$$

3.3 Trace preservation in the continuum

One of the defining features of the Lindblad equation, is the preservation of the trace of the reduced density matrix $\tilde{\rho}$. Let us first start with the coherent dynamics part of the Lindblad equation.

$$T_1 = \int d^3x \int d^3y \delta^{(3)}(\vec{x}-\vec{y})(i[\frac{\nabla_x{}^2}{M} + v(\vec{x})] - i[\frac{\nabla_y{}^2}{M} + v(\vec{y})])\rho(\vec{x},\vec{y},t) \quad (3.20)$$

We first observe that the potentials $v(\vec{x})$ and $v(\vec{y})$ will cancel each other due to the trace condition $\vec{x} = \vec{y}$. This means that we are left with the kinetic part, but for these to vanish, we need to be able to transform derivatives in x into derivatives in y. Luckily for us, this is something we are able to do, due to the presence of the delta function. Let us have a look how.

$$\int d^3x \int d^3y \delta^{(3)}(\vec{x}-\vec{y})(\frac{\partial^2}{\partial x_1^2} + \frac{\partial^2}{\partial x_2^2} + \frac{\partial^2}{\partial x_3^2} - \frac{\partial^2}{\partial y_1^2} - \frac{\partial^2}{\partial y_2^2} - \frac{\partial^2}{\partial y_2^2})\rho(\vec{x},\vec{y},t) \quad (3.21)$$

Using integration by parts, twice, on each of the six terms, we get

$$\int d^3x \int d^3y (\frac{\partial^2}{\partial x_1^2} + \frac{\partial^2}{\partial x_2^2} + \frac{\partial^2}{\partial x_3^2} - \frac{\partial^2}{\partial y_1^2} - \frac{\partial^2}{\partial y_2^2} - \frac{\partial^2}{\partial y_2^2}) \delta^{(3)}(\vec{x} - \vec{y}) \rho(\vec{x}, \vec{y}, t), \tag{3.22}$$

which we can do since we have periodic boundary conditions. Using the anti symmetry of the argument of the delta function, we can exchange a $\frac{\partial}{\partial x}$ with a $\frac{\partial}{\partial y}$ twice, and then using integration by parts again twice, we get

$$\int d^3x \int d^3y \delta^{(3)}(\vec{x} - \vec{y}) (\frac{\partial^2}{\partial y_1^2} + \frac{\partial^2}{\partial y_2^2} + \frac{\partial^2}{\partial y_3^2} - \frac{\partial^2}{\partial y_1^2} - \frac{\partial^2}{\partial y_2^2} - \frac{\partial^2}{\partial y_2^2}) \rho(\vec{x}, \vec{y}, t) \tag{3.23}$$

From this, the kinetic terms will vanish, and therefore $T_1 = 0$. Moving on to the F_1 terms.

$$T_2 = \int d^3x \int d^3y \delta^{(3)}(\vec{x} - \vec{y}) [2F_1(\frac{\vec{x} + \vec{y}}{2}) - 2F_1(\vec{0}) + F_1(\vec{x}) + F_1(\vec{y}) - 2F_1(\frac{\vec{x} + \vec{y}}{2})] \rho(\vec{x}, \vec{y}, t). \tag{3.24}$$

Here, due to the trace condition, $2F_1(\frac{\vec{x}+\vec{y}}{2})$ and $2F_1(\vec{0})$ will cancel each other out, and, $F_1(\vec{x})$ and $F_1(\vec{y})$ will together cancel out $2F_1(\frac{\vec{x}+\vec{y}}{2})$. This means that trace will vanish, IE. that $T_2 = 0$, for any choice of $D(\vec{r})$. There is a similar story to some of the F_2 terms.

$$T_3 = \int d^3x \int d^3y \delta^{(3)}(\vec{x} - \vec{y}) [2F_2(\vec{x}) - 2F_2(\frac{\vec{x} + \vec{y}}{2})] \nabla_x \rho(\vec{x}, \vec{y}, t) \tag{3.25}$$

will vanish due to the trace condition, and

$$T_4 = \int d^3x \int d^3y \delta^{(3)}(\vec{x} - \vec{y}) [2F_2(\vec{y}) - 2F_2(\frac{\vec{x} + \vec{y}}{2})] \nabla_y \rho(\vec{x}, \vec{y}, t) \tag{3.26}$$

will also vanish, independent of choice of $D(\vec{r})$. There are still two terms left including F_2, namely

$$T_5 = \int d^3x \int d^3y \delta^{(3)}(\vec{x} - \vec{y}) \{2F(\frac{\vec{x} - \vec{y}}{2})(\nabla_x - \nabla_y)\} \rho(\vec{x}, \vec{y}, t). \tag{3.27}$$

Recall that F_2 is dependent on first and third derivatives of $D(\vec{r})$. Also recall that for our case $D(\vec{r}) = g^2 T \int \frac{d^3k}{(2\pi)^3} \frac{\pi m_D^2 e^{i\vec{k}\cdot\vec{r}}}{k(k^2+m_D^2)^2}$. Ignoring the constants that go into the F_2 terms, the first derivative of $D(\vec{r})$ becomes

$$\vec{\nabla}_r D(\vec{r}) = k \int d^3k \frac{i\vec{k} e^{i\vec{k}\cdot\vec{r}}}{k(k^2 + m_D^2)} = k' \int d^3k \begin{bmatrix} \sin\theta\cos\phi \\ \sin\theta\sin\phi \\ \cos\theta \end{bmatrix} \frac{e^{i\vec{k}\cdot\vec{r}}}{(k^2 + m_D^2)} \tag{3.28}$$

We only need to check one coordinate, and choosing a suitable coordinate system, we obtain first obtain that $\vec{k} \cdot \vec{r} = kr\cos\theta$, and

$$\int dk d\theta d\phi \sin\theta \cos\theta \frac{e^{ikr\cos\theta}}{(k^2 + m_D^2)}. \tag{3.29}$$

$e^{ikr\cos\theta}$ will just be 1 since we are evaluating $\frac{\vec{x}-\vec{y}}{2}$ at $\vec{x} = \vec{y}$, which turns the argument into $\vec{0}$. This means that we can rewrite the integral in the following way

$$\int_{-1}^{1} y dy = 0 \tag{3.30}$$

The same argument follows also for the third derivative of F_2. This means that $2F_2(\frac{\vec{x}-\vec{y}}{2})$ is 0 for $\vec{x}-\vec{y}$, and also $T_5 = 0$.

$$T_6 = \int d^3x \int d^3y \delta^{(3)}(\vec{x}-\vec{y})\{2F_3^{ij}(\frac{\vec{x}-\vec{y}}{2})\frac{\partial}{\partial x_i}\frac{\partial}{\partial y_j} + \frac{1}{3}F_3^{kk}(\vec{0})\delta^{ij}\frac{\partial}{\partial x_i}\frac{\partial}{\partial x_j} + \frac{1}{3}F_3^{kk}(\vec{0})\delta^{ij}\frac{\partial}{\partial y_i}\frac{\partial}{\partial y_j}\}\rho(\vec{x},\vec{y},t) \quad (3.31)$$

As we saw earlier, we can transform second derivatives in x into second derivatives in y in the trace computation using integration by parts, we obtain

$$T_6 = \int d^3x \int d^3y \delta^{(3)}(\vec{x}-\vec{y})\{F_3^{ij}(\frac{\vec{x}-\vec{y}}{2})\frac{\partial}{\partial x_i}\frac{\partial}{\partial y_j} + \frac{1}{3}F_3^{kk}(\vec{0})\delta^{ij}\frac{\partial}{\partial x_i}\frac{\partial}{\partial x_j}\}\rho(\vec{x},\vec{y},t) \quad (3.32)$$

Again, we can turn one of the $\frac{\partial}{\partial x}$ into a $\frac{\partial}{\partial y}$, giving us

$$T_6 = \int d^3x \int d^3y \delta^{(3)}(\vec{x}-\vec{y})\{F_3^{ij}(\frac{\vec{x}-\vec{y}}{2}) - \frac{1}{3}F_3^{kk}(\vec{0})\delta^{ij}\}\frac{\partial}{\partial x_i}\frac{\partial}{\partial y_j}\rho(\vec{x},\vec{y},t), \quad (3.33)$$

which means that for the trace to vanish

$$F_3^{ij}(\vec{0}) - \frac{1}{3}F_3^{kk}(\vec{0})\delta^{ij} = 0. \quad (3.34)$$

Let us look at $F_3^{ij}(\vec{x})$. Recalling the definition of $F_3^{ij}(\vec{x}) = \frac{\partial}{\partial x_i}\frac{\partial}{\partial x_j}\frac{A(\vec{x})}{2M^2}$.

$$\frac{\partial}{\partial x_i}\frac{\partial}{\partial x_j}F_3^{ij}(\vec{r}) \mid_{\vec{r}=\vec{0}} = k' \int d^3k \frac{k_i k_j e^{i\vec{k}\vec{r}}}{k(k^2+m_D^2)} \quad (3.35)$$

First, we will be looking when $i \neq j$. First case, $i = x$, and $j = y$, will give us

$$k' \int dk d\theta d\phi k^3 \sin\theta[\sin\theta\cos\phi\sin\theta\sin\phi]\frac{e^{i\vec{k}\vec{r}}}{(k^2+m_D^2)} \quad (3.36)$$

Since the integral $\int_0^{2\pi} d\phi \cos\phi\sin\phi = 0$, the entire expression also vanishes. For the case $i = x$, and $j = z$, we will get

$$k' \int dk d\theta d\phi k^3 \sin\theta[\sin\theta\cos\phi\cos\theta]\frac{e^{i\vec{k}\vec{r}}}{(k^2+m_D^2)} \quad (3.37)$$

$\int_0^{2\pi} d\phi\cos\phi = 0$, again, the integral vanishes. The final case when $i = y$, and $j = z$, the integral will be

$$k' \int dk d\theta d\phi k^3 \sin\theta[\sin\theta\sin\phi\cos\theta]\frac{e^{i\vec{k}\vec{r}}}{(k^2+m_D^2)} \quad (3.38)$$

The same story here, $\int_0^{2\pi} d\phi \sin\phi = 0$, that integral will also vanish. Therefore, $F_3^{ij}(\vec{x}) = 0$ when $i \neq j$. Let us now check for the case when $i = j$, at $\vec{r} = 0$.

$$\frac{\partial^2}{\partial x_i^2}D(\vec{r}) = k' \int d^3k \frac{k_i^2 e^{i\vec{k}\cdot\vec{r}}}{k(k^2+m_D^2)} \quad (3.39)$$

Moving to Cartesian coordinates

$$k' \int dk_1 dk_2 dk_3 \frac{1}{\sqrt{k_1^2+k_2^2+k_3^2}} \frac{k_i^2}{(k_1^2+k_2^2+k_3^2+m_d^2)}$$

As we can see, this will be the same no matter what i is, it will be the same. This implies that

$$F_3^{ij}(\vec{0}) = \frac{1}{3} F_3^{kk}(\vec{0}) \tag{3.40}$$

and therefore $T_6 = 0$. Let us now have a look at

$$T_7 = \int d^3x \int d^3y \delta^{(3)}(\vec{x}-\vec{y})[2F_3^{ij}(\frac{\vec{x}+\vec{y}}{2})\frac{\partial}{\partial x_i}\frac{\partial}{\partial y_j} + F_3^{ij}(\vec{x})\frac{\partial}{\partial x_i}\frac{\partial}{\partial x_j} + F_3^{ij}(\vec{y})\frac{\partial}{\partial y_i}\frac{\partial}{\partial y_j}]\rho(\vec{x},\vec{y},t) \tag{3.41}$$

As we saw above, for our choice of $D(\vec{r})$, $F_3^{ij}(\vec{x}) = 0$ when $i \neq j$. This leaves us with three cases.

$$\int d^3x \int d^3y \delta^{(3)}(\vec{x}-\vec{y})[2F_3^{11}(\frac{\vec{x}+\vec{y}}{2})\frac{\partial}{\partial x_1}\frac{\partial}{\partial y_1} + F_3^{11}(\vec{x})\frac{\partial}{\partial x_1}\frac{\partial}{\partial x_1} + F_3^{11}(\vec{y})\frac{\partial}{\partial y_1}\frac{\partial}{\partial y_1}]\rho(\vec{x},\vec{y},t) \tag{3.42}$$

$$\int d^3x \int d^3y \delta^{(3)}(\vec{x}-\vec{y})[2F_3^{22}(\frac{\vec{x}+\vec{y}}{2})\frac{\partial}{\partial x_2}\frac{\partial}{\partial y_2} + F_3^{22}(\vec{x})\frac{\partial}{\partial x_2}\frac{\partial}{\partial x_2} + F_3^{22}(\vec{y})\frac{\partial}{\partial y_2}\frac{\partial}{\partial y_2}]\rho(\vec{x},\vec{y},t) \tag{3.43}$$

$$\int d^3x \int d^3y \delta^{(3)}(\vec{x}-\vec{y})[2F_3^{33}(\frac{\vec{x}+\vec{y}}{2})\frac{\partial}{\partial x_3}\frac{\partial}{\partial y_3} + F_3^{33}(\vec{x})\frac{\partial}{\partial x_3}\frac{\partial}{\partial x_3} + F_3^{33}(\vec{y})\frac{\partial}{\partial y_3}\frac{\partial}{\partial y_3}]\rho(\vec{x},\vec{y},t) \tag{3.44}$$

Let us introduce T_{7_1} as

$$\begin{aligned} T_{7_1} = \int d^3x \int d^3y \delta^{(3)}(\vec{x}-\vec{y})[&2F_3^{11}(\frac{\vec{x}+\vec{y}}{2})\frac{\partial}{\partial x_1}\frac{\partial}{\partial y_1} \\ &+ 2F_3^{22}(\frac{\vec{x}+\vec{y}}{2})\frac{\partial}{\partial x_2}\frac{\partial}{\partial y_2} + 2F_3^{33}(\frac{\vec{x}+\vec{y}}{2})\frac{\partial}{\partial x_3}\frac{\partial}{\partial y_3}]\rho(\vec{x},\vec{y},t) \end{aligned} \tag{3.45}$$

As T_{7_1} only depends on $\vec{x}+\vec{y}$ and $\vec{x}-\vec{y}$, we reparametrize in terms of $\vec{z}$ and $\vec{z}'$, where

$$\vec{z}' = \vec{x} - \vec{y} \tag{3.46}$$

$$\vec{z} = \vec{x} + \vec{y} \tag{3.47}$$

Introducing

$$\frac{\partial}{\partial x_i} = (\frac{\partial}{\partial z_i'} + \frac{\partial}{\partial z_i}) \tag{3.48}$$

$$\frac{\partial}{\partial y_i} = (\frac{\partial}{\partial z_i'} - \frac{\partial}{\partial z_i}) \tag{3.49}$$

$$\frac{\partial}{\partial z_i'} = \frac{1}{2}(\frac{\partial}{\partial x_i} + \frac{\partial}{\partial y_i}) \tag{3.50}$$

$$\frac{\partial}{\partial z_i} = \frac{1}{2}(\frac{\partial}{\partial x_i} - \frac{\partial}{\partial y_i}) \tag{3.51}$$

$$2\frac{\partial}{\partial x_i}\frac{\partial}{\partial y_i} = (\frac{\partial}{\partial x_i} + \frac{\partial}{\partial y_i})\frac{\partial}{\partial z_i'} - \frac{\partial^2}{\partial x_i^2} - \frac{\partial^2}{\partial y_i^2} \tag{3.52}$$

Plugging in into T_{7_1}will give us

$$T_{7_1} = \int d^3x \int d^3y \delta^{(3)}(\vec{z})\{F_3^{11}(\frac{\vec{z}'}{2})[(\frac{\partial}{\partial x_1}+\frac{\partial}{\partial y_1})\frac{\partial}{\partial z_1'} - \frac{\partial^2}{\partial x_1^2} - \frac{\partial^2}{\partial y_1^2}] + F_3^{22}(\frac{\vec{z}'}{2})[(\frac{\partial}{\partial x_2}+\frac{\partial}{\partial y_2})\frac{\partial}{\partial z_2'} - \frac{\partial^2}{\partial x_2^2} - \frac{\partial^2}{\partial y_2^2}] + F_3^{33}(\frac{\vec{z}'}{2})[(\frac{\partial}{\partial x_3}+\frac{\partial}{\partial y_3})\frac{\partial}{\partial z_3'} - \frac{\partial^2}{\partial x_3^2} - \frac{\partial^2}{\partial y_3^2}]\}\rho(\vec{x},\vec{y},t). \tag{3.53}$$

Inserting T_{7_1} back into T_7we obtain

$$T_7 = \int d^3x \int d^3y \delta^{(3)}(\vec{z})\{F_3^{11}(\frac{\vec{z}'}{2})(\frac{\partial}{\partial x_1}+\frac{\partial}{\partial y_1})\frac{\partial}{\partial z_1'} + F_3^{22}(\frac{\vec{z}'}{2})(\frac{\partial}{\partial x_2}+\frac{\partial}{\partial y_2})\frac{\partial}{\partial z_2'} + F_3^{33}(\frac{\vec{z}'}{2})(\frac{\partial}{\partial x_3}+\frac{\partial}{\partial y_3})\frac{\partial}{\partial z_3'}\}\rho(\vec{x},\vec{y},t). \tag{3.54}$$

Here we see that the $F_3^{ij}(\vec{x})$ and $F_3^{ij}(\vec{y})$ have been canceled by $2F(\frac{\vec{x}+\vec{y}}{2})$, though there is a remnant left of it. Integrating by parts on T_7 with respect to $\frac{\partial}{\partial z_i'}$, and using the fact that the delta function only depends on z_i and not z_i', we get

$$T_7 = -\int d^3x \int d^3y \delta^{(3)}(\vec{z})2\{\frac{\partial}{\partial z_1'}F_3^{11}(\frac{\vec{z}'}{2})(\frac{\partial}{\partial x_1}+\frac{\partial}{\partial y_1}) + \frac{\partial}{\partial z_2'}F_3^{22}(\frac{\vec{z}'}{2})(\frac{\partial}{\partial x_2}+\frac{\partial}{\partial y_2}) + \frac{\partial}{\partial z_3'}F_3^{33}(\frac{\vec{z}'}{2})(\frac{\partial}{\partial x_3}+\frac{\partial}{\partial y_3})\}\rho(\vec{x},\vec{y},t). \tag{3.55}$$

Let us introduce the A terms, written in terms of F_3^{ij}.

$$T_8 = \int d^3x \int d^3y \delta^{(3)}(\vec{x}-\vec{y})\{\nabla_x^2\frac{1}{2}F_3^{kk}(\vec{x}) + \nabla_y^2\frac{1}{2}F_3^{kk}(\vec{y}) + \vec{\nabla}_x 2F_3^{kk}(\vec{x})\vec{\nabla}_x + \vec{\nabla}_y 2F_3^{kk}(\vec{y})\vec{\nabla}_y\}\rho(\vec{x},\vec{y},t) \tag{3.56}$$

Let us go back to T_7 for a bit, where we will introduce a new variable $u_i = \frac{x_i+y_i}{2} = \frac{z_i}{2}$, $\frac{\partial}{\partial u_i} = 2\frac{\partial}{\partial z_i'}$. We get

$$T_7 = -\int d^3x \int d^3y \delta^{(3)}(\vec{z})\{+\frac{\partial}{\partial u_1}F_3^{11}(\vec{u}_1)\mid_{\vec{u}=\frac{\vec{x}+\vec{y}}{2}}(\frac{\partial}{\partial x_1}+\frac{\partial}{\partial y_1}) + \frac{\partial}{\partial u_2}F_3^{22}\mid_{\vec{u}=\frac{\vec{x}+\vec{y}}{2}}(\vec{u}_2)(\frac{\partial}{\partial x_2}+\frac{\partial}{\partial y_2}) + \frac{\partial}{\partial u_3}F_3^{33}\mid_{\vec{u}=\frac{\vec{x}+\vec{y}}{2}}($$

Adding T_7 and T_8, we obtain

$$T_{7+8} = \int d^3x \int d^3y \delta^{(3)}(\vec{z})\{-\frac{\partial}{\partial u_1}F_3^{11}(\vec{u}_1)\mid_{\vec{u}=\frac{\vec{x}+\vec{y}}{2}}(\frac{\partial}{\partial x_1}+\frac{\partial}{\partial y_1}) - \frac{\partial}{\partial u_2}F_3^{22}\mid_{\vec{u}=\frac{\vec{x}+\vec{y}}{2}}(\vec{u}_2)(\frac{\partial}{\partial x_2}+\frac{\partial}{\partial y_2}) - \frac{\partial}{\partial u_3}F_3^{33}\mid_{\vec{u}=\frac{\vec{x}+\vec{y}}{2}}(\vec{u}_3)(\frac{\partial}{\partial x_3}+\frac{\partial}{\partial y_3}) + \vec{\nabla}_x 2F_3^{kk}(\vec{x})\vec{\nabla}_x + \vec{\nabla}_y 2F_3^{kk}(\vec{y})\vec{\nabla}_y\}\rho(\vec{x},\vec{y},t) \tag{3.57}$$

Rewriting the nablas, we obtain

$$\begin{aligned} T_{7+8} = \int d^3x \int d^3y \delta^{(3)}(\vec{z})\{&-\frac{\partial}{\partial u_1}F_3^{11}(\vec{u}_1)\mid_{\vec{u}=\frac{\vec{x}+\vec{y}}{2}}(\frac{\partial}{\partial x_1}+\frac{\partial}{\partial y_1}) \\ &- \frac{\partial}{\partial u_2}F_3^{22}\mid_{\vec{u}=\frac{\vec{x}+\vec{y}}{2}}(\vec{u}_2)(\frac{\partial}{\partial x_2}+\frac{\partial}{\partial y_2}) - \frac{\partial}{\partial u_3}F_3^{33}\mid_{\vec{u}=\frac{\vec{x}+\vec{y}}{2}}(\vec{u}_3)(\frac{\partial}{\partial x_3}+\frac{\partial}{\partial y_3}) + \\ &\frac{\partial}{\partial x_1}(F_3^{11}+F_3^{22}+F_3^{33})\frac{\partial}{\partial x_1} + \frac{\partial}{\partial x_2}(F_3^{11}+F_3^{22}+F_3^{33})\frac{\partial}{\partial x_2} + \frac{\partial}{\partial x_3}(F_3^{11}+F_3^{22}+F_3^{33})\frac{\partial}{\partial x_3} \\ +\frac{\partial}{\partial y_1}(F_3^{11}+F_3^{22}+F_3^{33})\frac{\partial}{\partial y_1} + \frac{\partial}{\partial y_2}(F_3^{11}+F_3^{22}+F_3^{33})\frac{\partial}{\partial y_2} + \frac{\partial}{\partial y_3}(F_3^{11}+F_3^{22}+F_3^{33})\frac{\partial}{\partial y_3}&\}\rho(\vec{x},\vec{y},t) \end{aligned} \tag{3.58}$$

Let us have a look at $\nabla_i\nabla_j\nabla_j D(\vec{r})$. This is, based on or dissipative kernel

$$\nabla_i\nabla_j\nabla_j D(\vec{r}) = k' \int d^3k \frac{k_j^2 k_i e^{i\vec{k}\cdot\vec{r}}}{k(k^2+m_D^2)} \tag{3.59}$$

Going through all the different combinations of $k_j^2 k_i$ will yield that for $i \neq j$, $\nabla_i\nabla_j\nabla_j D(\vec{0}) = 0$. Therefore, we get that $\frac{\partial}{\partial x_i}(F_3^{11}+F_3^{22}+F_3^{33})\frac{\partial}{\partial x_i} = \frac{\partial}{\partial x_1}(F_3^{11})\frac{\partial}{\partial x_1}$. Same applies to all the other coordinates as well. Rewriting T_7 as

$$\sum_i \frac{\partial}{\partial x_i}(F_3^{kk}(\vec{x}))\frac{\partial}{\partial x_i} + \frac{\partial}{\partial y_i}(F_3^{kk}(\vec{y}))\frac{\partial}{\partial y_i} \tag{3.60}$$

Rewriting in terms of z_i and z_i'

$$\sum_i (\frac{\partial}{\partial z_i'}+\frac{\partial}{\partial z_i})(F_3^{kk}(\frac{\vec{z_i}'+\vec{z_i}}{2}))(\frac{\partial}{\partial z_i'}+\frac{\partial}{\partial z_i}) + (\frac{\partial}{\partial z_i'}-\frac{\partial}{\partial z_i})(F_3^{kk}(\frac{\vec{z_i}'-\vec{z_i}}{2}))(\frac{\partial}{\partial z_i'}-\frac{\partial}{\partial z_i}) \tag{3.61}$$

Using the fact that in the trace, we can turn $\frac{\partial}{\partial z_i}$ into $\frac{\partial}{\partial z_i'}$, and then integrating by parts, we get

$$-\sum_i 2F_3^{kk}(\frac{\vec{z_i}'+\vec{z_i}}{2})\frac{\partial}{\partial z_i'}(\frac{\partial}{\partial z_i'}+\frac{\partial}{\partial z_i}) - 2F_3^{kk}(\frac{\vec{z_i}'-\vec{z_i}}{2})\frac{\partial}{\partial z_i'}(\frac{\partial}{\partial z_i'}-\frac{\partial}{\partial z_i}) \tag{3.62}$$

Using the trace condition $z_i = 0$,we obtain

$$-\sum_i 4F_3^{kk}(\frac{\vec{z_i}'}{2})\frac{\partial}{\partial z_i'}\frac{\partial}{\partial z_i'} \tag{3.63}$$

We can finally combine everything together to see that the trace vanish

$$\begin{aligned}\frac{1}{2}\sum_i \frac{\partial^2}{\partial x_i^2}F_3^{kk}(\vec{x}) + \frac{\partial^2}{\partial y_i^2}F_3^{kk}(\vec{y}) = \frac{1}{2}\sum_i \{&(\frac{\partial}{\partial z_i}\frac{\partial}{\partial z_i} + \frac{\partial}{\partial z_i}\frac{\partial}{\partial z_i'} + \frac{\partial}{\partial z_i'}\frac{\partial}{\partial z_i} + \frac{\partial}{\partial z_i'}\frac{\partial}{\partial z_i'})F_3^{kk}(\frac{\vec{z_i'}+\vec{z_i}}{2}) \\ &+ (\frac{\partial}{\partial z_i}\frac{\partial}{\partial z_i} - \frac{\partial}{\partial z_i}\frac{\partial}{\partial z_i'} - \frac{\partial}{\partial z_i'}\frac{\partial}{\partial z_i} - \frac{\partial}{\partial z_i'}\frac{\partial}{\partial z_i'})F_3^{kk}(\frac{\vec{z_i'}-\vec{z_i}}{2})\end{aligned} \tag{3.64}$$

This turns into

$$2\sum_i \{(\frac{\partial}{\partial z_i'}\frac{\partial}{\partial z_i'})F_3^{kk}(\frac{\vec{z_i'}+\vec{z_i}}{2}) + (\frac{\partial}{\partial z_i'}\frac{\partial}{\partial z_i'})F_3^{kk}(\frac{\vec{z_i'}-\vec{z_i}}{2})\} \tag{3.65}$$

Integrating by parts gives us

$$\sum_i \{2F_3^{kk}(\frac{\vec{z_i'}+\vec{z_i}}{2})\frac{\partial}{\partial z_i'}\frac{\partial}{\partial z_i'} + 2F_3^{kk}(\frac{\vec{z_i'}-\vec{z_i}}{2})\frac{\partial}{\partial z_i'}\frac{\partial}{\partial z_i'}\} \tag{3.66}$$

Using $z_i = 0$, we get

$$\sum_i 4F_3^{kk}(\frac{\vec{z_i}'}{2})\frac{\partial}{\partial z_i'}\frac{\partial}{\partial z_i'} \tag{3.67}$$

Which we see that is the exact opposite as the remnant of the F_3^{ij} terms. And by that we can conclude that the trace is indeed preserved. To summarize, we have found out, that our F_3^{ij} terms have these properties:

$$F_3^{ij}(\vec{x}) = \delta^{ij}F_3^{kk}(\vec{x}) \tag{3.68}$$

$$F_3^{11}(\vec{0}) = F_3^{22}(\vec{0}) = F_3^{33}(\vec{0}) \tag{3.69}$$

$$\frac{\partial}{\partial x_1}(F_3^{11} + F_3^{22} + F_3^{33}) = \frac{\partial}{\partial x_1}F_3^{11} \tag{3.70}$$

$$\frac{\partial}{\partial x_2}(F_3^{11} + F_3^{22} + F_3^{33}) = \frac{\partial}{\partial x_2}F_3^{22} \tag{3.71}$$

$$\frac{\partial}{\partial x_3}(F_3^{11} + F_3^{22} + F_3^{33}) = \frac{\partial}{\partial x_3}F_3^{33} \tag{3.72}$$

4 Numerics and discretization

4.1 RN-SBP operator

Why cannot we use the regular finite difference operators $\mathbb{D}^{Old}_{x_k}$ and $\mathbb{D}^{Old}_{y_k}$ to build $\mathbb{D}^{Old}_{z_k}$ and $\mathbb{D}^{Old}_{z'_k}$? Assuming that we have the same spacing in all direction $\Delta x_k = \Delta y_k = \Delta$, and with some abuse of notation

$$\begin{aligned}\frac{1}{2}(\mathbb{D}^{Old}_{x_k} + \mathbb{D}^{Old}_{y_k})f(\vec{x},\vec{y}) &= \frac{1}{4\Delta}(f(x_k+\Delta,y_k) - f(x_k-\Delta,y_k) + f(x_k,y_k+\Delta) - f(x_k,y_k+\Delta)) \\ &\neq \mathbb{D}^{Old}_{z'_k} f(\vec{x},\vec{y}) = \frac{1}{2\Delta_z}(f(x_k+\frac{\Delta_z}{2},y_k+\frac{\Delta_z}{2}) - f(x_k-\frac{\Delta_z}{2},y_k-\frac{\Delta_z}{2})) \quad (4.1)\end{aligned}$$

As this is clearly not what we are looking for, we need to construct new finite difference operators that do fulfill the reparametrization. To start, we have ordered our density matrix in such a way that

$$\rho = \begin{bmatrix} \rho(x_{0,0,0},y_{0,0,0}) \\ \rho(x_{0,0,0},y_{0,0,1}) \\ \vdots \\ \rho(x_{0,0,0},y_{0,1,0}) \\ \vdots \\ \rho(x_{0,0,1},y_{0,0,0}) \\ \vdots \\ \rho(x_{1,1,1},y_{1,1,1}) \\ \vdots \\ \rho(x_{N-1,N-1,N-1},y_{N-1,N-1,N-1}) \end{bmatrix} \quad (4.2)$$

i.e., we are always shifting y_3 one up, then, as we reach the box size, shifting then y_2 one up, and etc. for all coordinates in our six dimensional space. Introducing the shift operators S_+ and S_-, which when we have periodic boundary conditions will be

$$S_+ = \begin{bmatrix} 0 & 0 & 0 & \dots & 0 & 1 \\ 1 & 0 & 0 & & 0 & 0 \\ 0 & 1 & 0 & & 0 & 0 \\ 0 & 0 & 1 & & 0 & 0 \\ \vdots & \vdots & 0 & \ddots & \vdots & \vdots \\ 0 & 0 & \dots & 0 & 1 & 0 \end{bmatrix} \quad (4.3)$$

$$S_- = S_+^T \quad (4.4)$$

S_+will shift us upwards in the in the grid, and S_- will shift us downwards in the grid. $S_+ + S_- = \mathbb{1}$

$$Q = -S_+ + S_- = \begin{bmatrix} 0 & 1 & & & -1 \\ -1 & 0 & & & \\ & -1 & \ddots & 1 & \\ & & & 0 & 1 \\ 1 & & & -1 & 0 \end{bmatrix} \quad (4.5)$$

where $D \equiv H^{-1}Q$. $H = \Delta\mathbb{1}$ is the integration prescription. Trivially, $Q + Q^T = 0$ One can show[10] that the summation by parts, or SBP, property will be $(u, Dv)_H = -(Du, v)_H$. For the

reparametrizatrion condition to be fulfilled, we need to create a finite difference operator that evaluates at all the neighboring corners. How do we do that? We will do that by essentially shifting the old finite difference operator, in for example the x_1 direction, along the y_1 one up and one down, do the old finite difference operator at those two points, and average the result together. We will then construct our new finite difference operators $\mathbb{D}_{x_k}$ and $\mathbb{D}_{y_k}$ as

$$\mathbb{D}_{x_k} = (D \otimes S_+ + D \otimes S_-) \tag{4.6}$$

$$\mathbb{D}_{y_k} = (S_+ \otimes D + S_- \otimes D) \tag{4.7}$$

These are the RN-SBP operators. As for the explicit representation of the $\mathbb{D}_{x_k}$ and $\mathbb{D}_{y_k}$acting on ρ is, using the same abuse of notation as before

$$\mathbb{D}_{x_k}\rho(\vec{x},\vec{y}) = \frac{1}{2}(\frac{\rho(x_k+1,y_k+1)-\rho(x_k-1,y_k+1)}{2\Delta} + \frac{\rho(x_k+1,y_k-1)-\rho(x_k-1,y_k-1)}{2\Delta}) \tag{4.8}$$

$$\mathbb{D}_{y_k}\rho(\vec{x},\vec{y}) = \frac{1}{2}(\frac{\rho(x_k+1,y_k+1)-\rho(x_k+1,y_k-1)}{2\Delta} + \frac{\rho(x_k-1,y_k+1)-\rho(x_k-1,y_k-1)}{2\Delta}) \tag{4.9}$$

We define the reparametrizations $z_k = (x_k + y_k)$ and $z'_k = (x_k - y_k)$ in the same way that we did in the continuum

$$\mathbb{D}_{z_k}\rho(\vec{x},\vec{y}) = \frac{1}{2}(\mathbb{D}_{x_k} - \mathbb{D}_{y_k}) \tag{4.10}$$

$$\mathbb{D}_{z'_k}\rho(\vec{x},\vec{y}) = \frac{1}{2}(\mathbb{D}_{x_k} + \mathbb{D}_{y_k}) \tag{4.11}$$

Evaluating it explicitly, we obtain

$$\mathbb{D}_{z_k}\rho(\vec{x},\vec{y}) = \frac{\rho(x_k-1,y_k+1)-\rho(x_k+1,y_k-1)}{2\Delta} \tag{4.12}$$

$$\mathbb{D}_{z'_k}\rho(\vec{x},\vec{y}) = \frac{\rho(x_k+1,y_k-1)-\rho(x_k-1,y_k+1)}{2\Delta} \tag{4.13}$$

Suppose we have two functions, u and v, where u only depends on z' and v only on z.

$$\mathbb{D}_{z_k}(u \circ v) = u \circ \mathbb{D}_{z_k} v \tag{4.14}$$

$$\mathbb{D}_{z'_k}(u \circ v) = v \circ \mathbb{D}_{z'_k} u \tag{4.15}$$

Though we have by created a finite difference operator that by construction is reparametrization neutral, it has value in showing explicitly that it preserves the trace preservation. First, the ability to transform a derivative in x into one in y with the help of the delta function

$$\mathbb{D}_{x_k}\delta(\vec{x}-\vec{y}) = (\mathbb{D}_{z'_k} + \mathbb{D}_{z_k})\delta(\vec{z}) = (-\mathbb{D}_{z'_k} + \mathbb{D}_{z_k})\delta(\vec{z}) = -\mathbb{D}_{y_k}\delta(\vec{x}-\vec{y}) \tag{4.16}$$

Another computation in the trace that was performed, was in T_7, where we needed to reparametrize it

$$\begin{aligned} 2\mathbb{D}_{x_k}\mathbb{D}_{y_k} &= [(\mathbb{D}_{x_k} + \mathbb{D}_{y_k})(\mathbb{D}_{x_k} + \mathbb{D}_{y_k}) - \mathbb{D}_{x_k}^2 - \mathbb{D}_{y_k}^2] \\ &= [2(\mathbb{D}_{x_k} + \mathbb{D}_{y_k})\mathbb{D}_{z'_k} - \mathbb{D}_{x_k}^2 - \mathbb{D}_{y_k}^2] \end{aligned} \tag{4.17}$$

As we saw in the start of this subsection, if we had used the old finite difference operators, this step would no longer have been valid. The last manipulation we did in the trace preservation, was

$$\mathbb{D}_{z'_K}(\delta(z_k) \circ F_3(\frac{z'_k}{2})) = \delta(z_k) \circ \mathbb{D}_{z'_k}(F_3(\frac{z'_k}{2}) \tag{4.18}$$

As seen above, this also holds. We have now created a new finite difference operator, the RN-SBP operator, that does preserve the trace.

For a more thorough introduction to SBP operators, see for example [16].

4.2 Crank-Nicholson method

The time evolution of the system is given by $\frac{\partial}{\partial t}\tilde{\rho} = e^{iM\Delta t}$. Naively, one would first try to Taylor expand the exponential, such that it gives us

$$\tilde{\rho}(t+\Delta t) = (1+iM\Delta t)\tilde{\rho}(t). \tag{4.19}$$

But as we can see, the norm of the system is no longer preserved, as $|(1+iM\Delta t)| \neq 1$. That was the forward time stepping. We could also have done the backwards time stepping,

$$(1-iM\Delta t)\tilde{\rho}(t+\Delta t) = \tilde{\rho}(t). \tag{4.20}$$

Again we have the same issue. But, if we combine these two together, first stepping halfway forwards in time from the current time, and then halfway back in time from the next step, into

$$(1-iM\frac{\Delta t}{2})\tilde{\rho}(t+\Delta t) = (1+iM\frac{\Delta t}{2})\tilde{\rho}(t), \tag{4.21}$$

or equivalently

$$\tilde{\rho}(t+\Delta t) = \frac{(1+iM\frac{\Delta t}{2})}{(1-iM\frac{\Delta t}{2})}\tilde{\rho}(t). \tag{4.22}$$

This is now norm preserving as $|\frac{(1+iM\frac{\Delta t}{2})}{(1-iM\frac{\Delta t}{2})}| = 1$.

So, why go with the Crank-Nicholson method? The Crank-Nicholson preserves both hermiticity, and positivity, in addition, if employed with the new derivative operator, also the trace[10]. It does have the issue of being more computational heavy compared to other methods, but the benefits listed above outweigh the slower performance.

5 Simulation results and discussions

We've come to section were we will be getting some results from the code we have written. We ran the coherent dynamics simulation once, the recoiless limit twice, at $T = 0.1M$ and $T = 0.3M$, and the full Lindblad simulation was ran three times, with $T = 0.1M$, $T = 0.3M$, and one with more different simulation parameters, with will be mentioned later.

Our density matrix is expressed in the eigenstate basis,

$$\rho_{nm}(t) = \int dx \int dy \, \langle \psi_n(x) | \rho(x, y, t) | \psi_m(x) \rangle \tag{5.1}$$

$$\rho_{nm}(t) = \int dx \int dy \, \langle \psi_n | x \rangle \, \langle x | \psi_k \rangle \, \langle \psi_k | y \rangle \, \langle y | \psi_m \rangle \tag{5.2}$$

We read of the survival probability P_n as the diagonal entries of the density matrix $P_n = \rho_{nn}$. Energy of the system is computed as $\langle E \rangle = Tr[H_P \rho]$

5.1 Simulation parameters and numerical tolerances

5.1.1 Numerical step sizes and tolerances

For all of the simulations, we used 8 grid points per dimension, as that was the highest possible we could go, when using $16GB$ of memory. The spatial step size Δx was set at $\Delta x = 1$, and the temporal step size Δt was set at $\Delta t = 0.1$. Regarding the numerical tolerances, for all simulations, it was set at $\Delta_{GMRES} = 10^{-12}$ for the GMRES algorithm, and the max number of iterations for the solver was set at $N_{GMRES} = 1000$. The number of iterations for the quarkonium simulation itself, was set at 5000 iterations for all cases. This fairly low was set to avoid too lengthy simulations, due to the limited available computing power we had at our disposable.

5.1.2 Simulation parameters

All simulations ran using a Gaussian dissipative kernel

$$D(\vec{r}) = \gamma e^{-\frac{\vec{r}^2}{l_{cor}^2}}, \tag{5.3}$$

and the Cornell potential

$$v(\vec{r}) = -\frac{\alpha}{\vec{r}} + \sigma \vec{r} + c. \tag{5.4}$$

The values for α, σ and c was set at $\alpha = 0.3$, $\sigma = 0.03248$ and $c = 0$ respectively. These values for the potential comes are from first principle calculations from lattice QCD(?)[2]. The other simulation parameters were chosen to correspond as closely as possible to [10], as to allow as accurate comparison of the 1D simulation to the 3D simulation as possible. Therefore, γ was set at $\frac{T}{\pi}$, and the correlation length l_{cor} was $\frac{\Delta x}{T}$. Mass of the quarkonium particle was set at $m = 0.479188$. The initial density matrix was initialized with 100% ground state in all simulations.

5.2 Coherent dynamics

As a first test of the code, we ran only the coherent dynamics part of the Lindblad equation

$$\frac{\partial}{\partial t}\rho(x, y, t) = i[\frac{\nabla_x^2}{M} + v(\vec{x})]\rho(\vec{x}, \vec{y}, t) - i[\frac{\nabla_y^2}{M} + v(\vec{y})]\rho(\vec{x}, \vec{y}, t). \tag{5.5}$$

This is essentially just the Schrödinger equation for the density matrix. It serves as an important milestone in the project, as it allows us to make sure that the coherent dynamics works, not just alone, but also for the recoiless limit and the full Lindblad equation.

What do we expect to see from the coherent dynamics? The ground state is a stationary state, and the Schrödinger equation cannot transform one stationary state to another on. Since the density matrix was initialized with 100% ground state, we expect the system to stay that way. It's a similar story for the total energy of the system. As there is no medium for the system to gain or shed energy, we would expect the energy to stay constant during the entire simulation. As for the trace, as we showed in the trace preservation part, the trace should also remain unity.

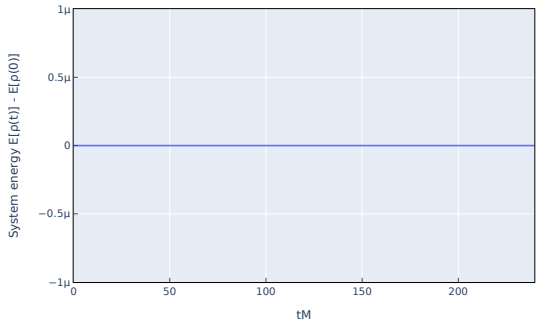

Figure 1: Coherent dynamics, system energy

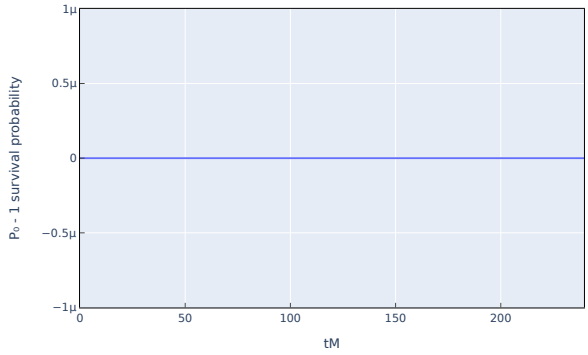

Figure 2: Coherent dynamics, survival probability for P_0

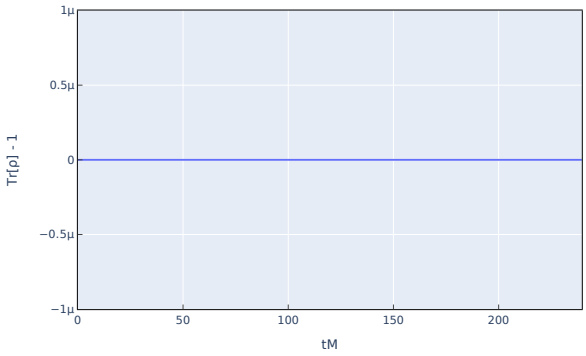

(a) Trace, absolute value

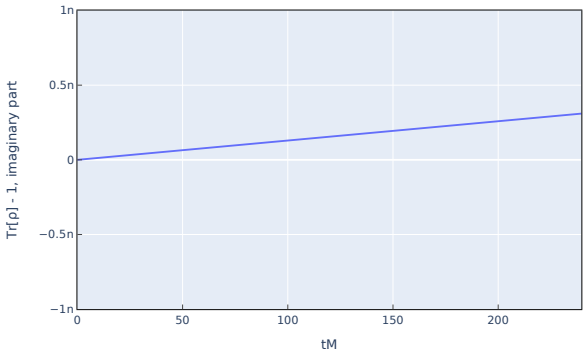

(b) Trace, imaginary component

Figure 3: Coherent dynamics, trace

How do the result we got, compare to what we expect? Looking at the survival probability of the ground state, we see no deviation from the expected value of 100%. The energy tells us the same story. There is no energy deviation from the initial energy of the density matrix over the run of the simulation, just as we expected. The absolute value of the trace stays at unity, within machine precision, for the entirety of the simulation. The imaginary part of the trace starts on the order of 10^{-13}, and after 5000 iterations, it is at the order of 10^{-10}, which is what we would expect when using a tolerance of 10^{-12}. We can therefore, based on these results, the coherent dynamics part of the code works as intended, and produces the results we would expect. We can then move on the recoiless limit.

5.3 Recoiless limit approximation

The second results that we got, was for the recoiless limit approximation of the Lindblad equation. This limit is when we are leaving out all the A terms, F_2 terms, the F_3^{ij} terms, and all parts of F_1 besides $D(\vec{r})$. The Lindblad equation will then look like

$$\frac{\partial}{\partial t}\rho(x,y,t) = i[\frac{\nabla_x^2}{M} + v(\vec{x})]\rho(\vec{x},\vec{y},t) - i[\frac{\nabla_y^2}{M} + v(\vec{y})]\rho(\vec{x},\vec{y},t) \\ + [2D(\frac{\vec{x}-\vec{y}}{2}) - 2D(\vec{0}) + D(\vec{x}) + D(\vec{y}) - 2D(\frac{\vec{x}+\vec{y}}{2})]\rho(x,y,t). \quad (5.6)$$

The recoiless limit ignores all dissipative effects on the quarkonium, and thus only have fluctuations. This means that the quarkonium would only take up energy, and never shed any of it away.

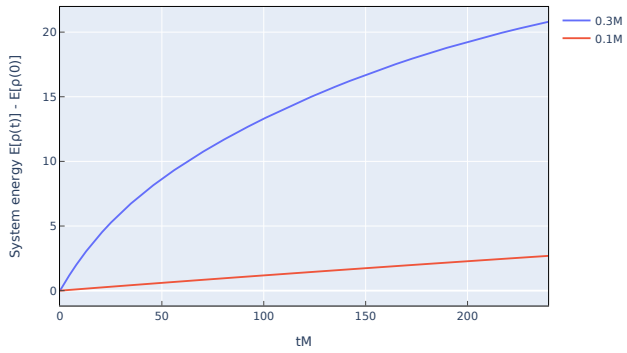

Figure 4: Recoiless limit, system energy

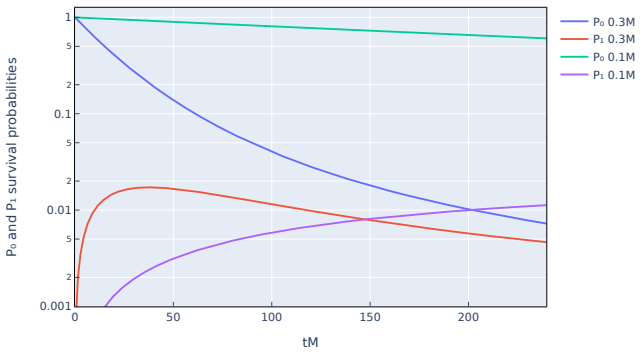

Figure 5: Recoiless limit, survival probabilities

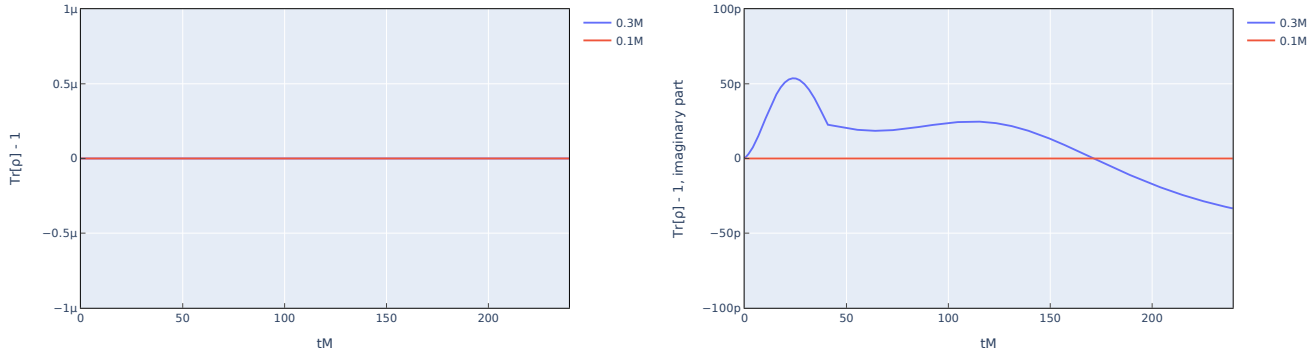

(a) Trace, absolute value

(b) Trace, imaginary component

Figure 6: Recoiless limit, trace

When $T = 0.3M$, we see a fairly rapid heating of the system, with a peak P_1 at $tM = 37$. The reason for the peak, is that, as the system picks up more and more energy, some of the ground

state will excite into the first excited state. As the system continuous to take up energy from the environment, some of the first excited states will either jump up into a higher state, or melt away. This is why we see a drop in P_1 after a certain point. We do believe the same will happen at $T = 0.1M$, though the simulation was performed long enough to observe this happening. As for the relative difference in the survival probabilities between $T = 0.1M$ and $T = 0.3M$, this is explained by the Boltzmann factor

$$\frac{P_j}{P_i} = e^{\frac{E_i - E_j}{kT}}. \tag{5.7}$$

As the temperature T increases, the ratio between the different survival probabilities will shrink, which is what we do observe. Though the simulation length is on the short end, it does not look like the system is able to thermalize, just as we would expect, since the system has no way of shedding any energy back into the environment. Regarding the energy, one would naively expect the energy to grow to infinity, as the system is taking up more and more energy from the environment. This is not quite what we are seeing, as the energy increase is steadily decreasing, suggesting that it will converge at some point. The reason we are not surprised seeing this, is that it reaches an infinite temperature limit on a finite lattice[10].

The trace is also excellently preserved in the recoiless limit. There is a somewhat mysterious behavior of the imaginary component of the trace. We would expect it to rise or decrease linearly, with the slope depending on the tolerances used. What we see is a quite erratic behavior, with even a discontinuity at around $tM = 45$, though all of it are within machine precision level. We cannot explain why the imaginary part of the trace behaves in this erratic fashion, but it is most likely related to some numerical imprecision.

In an infinite box, we would expect the survival probabilities in the recoiless limit to approach 0 for $t(\infty)$. If we are looking at the Boltzmann distribution

$$F(E) = Ae^{-\frac{E}{kT}} \tag{5.8}$$

where A is a normalization constant. During the normalization procedure, one has to divide by the sum over all states. With an infinite box, the normalization procedure would require a division by infinity, such that, indeed, the survival probability for any state would go towards zero. In a finite box, however, the normalization procedure will longer have a division by infinity, but some finite number. Therefore, we would expect the survival probabilities to go to some small, but non zero number.

Overall, the recoiless limit exhibits the behavior that we would expect, and we can then move on to the full simulation of the Lindblad equation.

5.4 Full Lindblad equation

Coming to the simulation of the full we do know from beforehand testing of the code, that the trace is not preserved properly. We also know where the cause of the non preserved trace is. In the trace preservation calculations, we saw that we had to discretize the A terms

$$-[\frac{(\nabla_x^2)^2 A(\vec{x})}{4M^2} + \frac{(\nabla_y^2)^2 A(\vec{y})}{4M^2}]\rho(\vec{x}, \vec{y}, t) \tag{5.9}$$

and

$$-[\nabla_x \frac{(\nabla_x^2) A(\vec{x})}{M^2} \nabla_x + \nabla_y \frac{(\nabla_x^2) A(\vec{y})}{M^2} \nabla_y]\rho(\vec{x}, \vec{y}, t) \tag{5.10}$$

in a particular way, such that they cancel out with some remaining F_3^{ij} terms

$$[2F_3^{ij}(\frac{\vec{x} + \vec{y}}{2})\frac{\partial}{\partial x_i}\frac{\partial}{\partial y_j} + F_3^{ij}(\vec{x})\frac{\partial}{\partial x_i}\frac{\partial}{\partial x_j} + F_3^{ij}(\vec{y})\frac{\partial}{\partial y_i}\frac{\partial}{\partial y_j}]\rho(\vec{x}, \vec{y}, t) \tag{5.11}$$

We do know from debugging that the rest of the F_3^{ij}, and the F_2 do preserve the trace, as shown in the trace preservation, we can with high confidence that it is here the issues is.

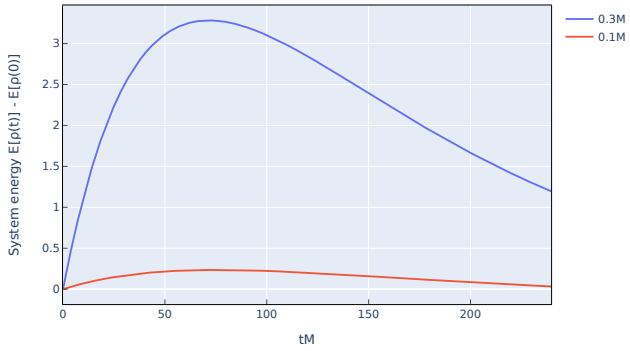

Figure 7: Full Lindblad equation, system energy

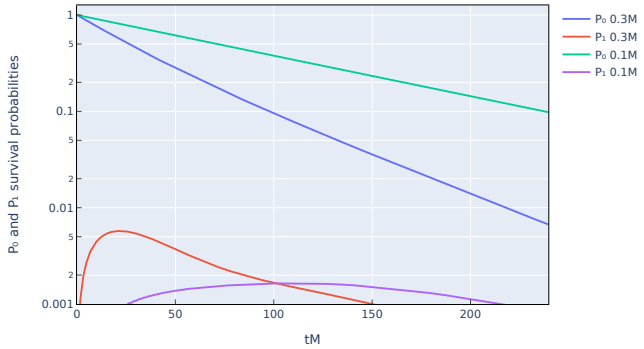

Figure 8: Full Lindblad equation, survival probabilities

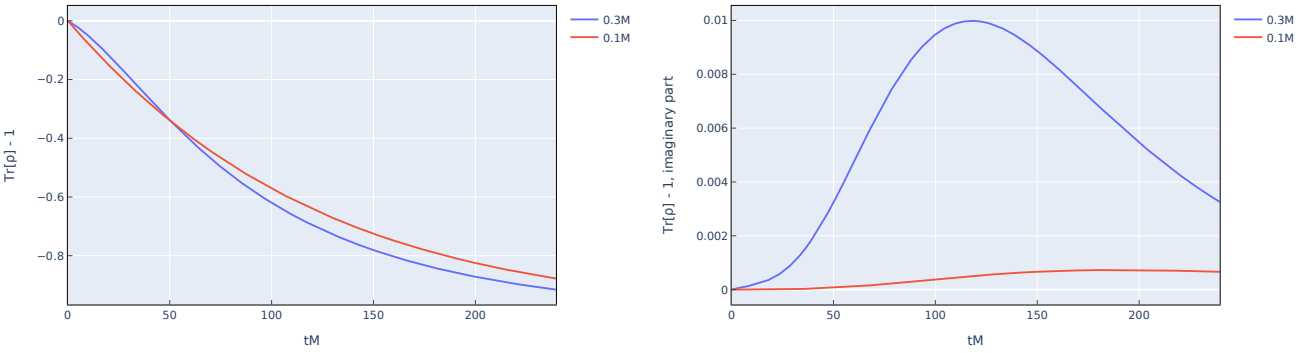

(a) Trace, absolute value

(b) Trace, imaginary component

Figure 9: Full Lindblad equation, trace

As we can see from the plots, there is a quite significant decrease of the trace, even in this relatively short simulation. The loss of the trace is equivalent to loosing probability, which we see quite clearly in the survival probabilities of the different states, in both of the simulations. We also see this in the energy, which is also calculated from the trace. We would expect it to converge to a fixed value as the system thermalizes, but it starts to decrease fairly rapidly as the trace is shrinking.

We do in the beginning, see a rapid heating of the system when $T = 0.3M$, and a much slower heating when $T = 0.1M$, with P_1, when $T = 0.3M$, reaches it's peak at roughly $tM = 20$, before it starts to drop, quite quickly, due to the non preservation of the trace.

As the decrease of the trace was quite severe, we did a final simulation, decreasing the strength of the interaction to try to tame the trace. The simulation parameters we choose for this run was, $T = 0.2$, $\gamma = 0.01$, and $l_{cor} = 2ds$, with the rest of the parameters and tolerances being the same as all the previous simulations.

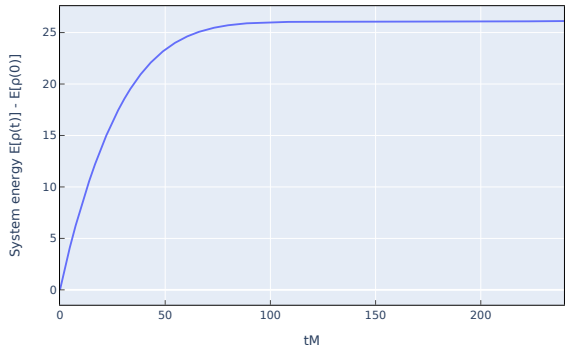

Figure 10: Full Lindblad equation, $\gamma = 0.01$, system energy

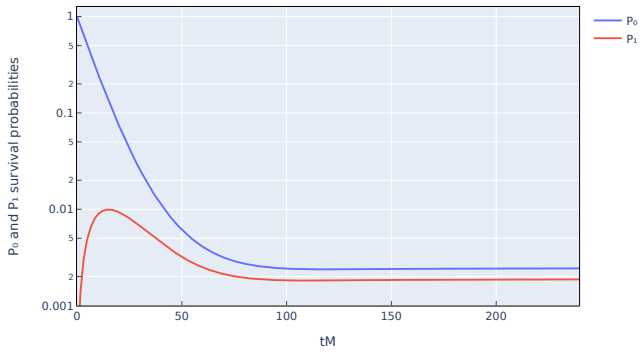

Figure 11: Full Lindblad equation, $\gamma = 0.01$, survival probabilities

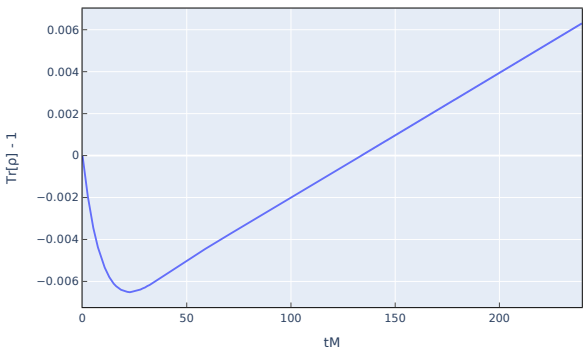

(a) Trace, absolute value

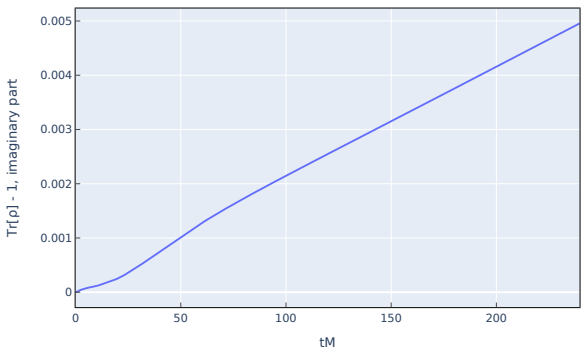

(b) Trace, imaginary component

Figure 12: Full Lindblad equatuin, $\gamma = 0.01$, trace

The systems heats up quite rapidly, with P_1 peaking at $tM = 15$. The system also thermalizes fairly quickly, reaching thermal equilibrium at roughly $tM = 100$, with a minimum at $tM = 111$. The survival probabilities, will then start to rise, as a consequence of the non preserved, rising trace. There is a similar story with the energy, reaching equilibrium at the same point.

We recognize from this three simulations, that, in particular, γ, the strength of the interaction between the system and the environment, has a significant impact on the trace, when it is not conserved.

6 Conclusions and outlook

As far as I can tell, there have been no equivalently done simulations with other approaches in the three dimensional case, only in the one dimensional case. When the discretization of the A terms have been fixed, and done correctly, this will den serve as a comparison towards other, more computational efficient approaches, such as the stochastic unraveling of the master equation is done.

We would have liked to compare the recoiless limit with the full Lindblad equation, at the same parameters, as to see if, and when, the recoiless is a good approximation for the full Lindblad equation. This is out of the question, due to the complete breakdown of the simulation of the full Lindblad equation.

As a comparison with the one dimensional case of the Lindblad equation[10], though, not entirely applicable due to the usage of the Cornell potential in the 3D version, as compared to the Yukawa potential employed in the 1D case, we see the same behavior for the recoiless limit, and the behavior that we would expect. We are therefore confident in the validity of the recoiless approximation of the code. As far as the full simulation, due to the incorrect discretization of the A terms in the 3D code, it is more difficult to compare these two results with one another. This can be done when the proper discretization of the A terms is implemented in the 3D code.

In conclusion, we have showed that the trace of the density matrix will be preserved using the RN-SBP, at least for our particular choice of $D(\vec{r})$. In addition, we've also seen the importance of the preservation of the trace, and how changes to how the system is coupled to the medium has an effect on the trace of the density matrix. Both the coherent part, and the recoiless limit of the code works as intended. The only thing left, is to fix the wrongly discretized A terms, such that we can get the full Lindblad equation simulated.

Though effort has gone into this project, by no means is the work done. The most pressing concern would be that of the incorrectly discretized A terms. Once those are implemented, we have a more solid base for any future comparison, with for example the 1D code, as to make sure that the 3D version is actually correct. Another improvement that can be done is to implement the real time static potential for hot QCD[8], in addition to the current Gaussian dissipative kernel that is already implemented. In addition, the half box size periodic boundary conditions for the dissipative is not implemented in the code. However, to get a truly better simulation, one would need to significantly increase the grid size of the simulation. With $16GB$ of RAM, the current maximum number of grid points in a single direction would be 8, in comparison to the one dimensional case ability to easily run 256 grid points per dimension on the same memory budget. As a rough estimation, for the same number of grid points, 256, in the three dimensional case, we would need approximately $4PB$ of memory just to house the density matrix vector itself, using double precision floating point numbers. This is not even taking the operator matrix in consideration. This is unfeasible in the near future, so we would need to make use of other methods to keep the memory usage to a manageable level. One such possibility would be that of the PETSc matrix free methods, to limit the usage of memory. Other more minor changes to the code that could be implemented, is a check of hermiticity and positivity of the density matrix. Though, if we ignore the broken A terms, and look at the recoiless limit, the fact that it gives us the expected results, suggest that it does not violate both of them, though, we cannot be certain of it without actually doing the check of it.

As for improvements related to the physics side of things, one could check if any of founding assumptions that went into creating the master equation are valid. Is the markovian approximation a good approximation? When does it break down? What about the non-relativistic behavior of the quarkonium we have assumed?

We hope that in the near future, we can fix the discretized A terms, such that we can get an

accurate simulation of the system, which in turn can be helpful as a cross-check between other, less computational heavy methods.

Acknowledgments

I would like to thank Dr. Alexander Karl Rothkopf for supervising this project with me.

References

[1] Yukinao Akamatsu. Heavy quark master equations in the lindblad form at high temperatures. *Physical Review D*, 91(5), mar 2015.

[2] Yannis Burnier, Olaf Kaczmarek, and Alexander Rothkopf. Quarkonium at finite temperature: towards realistic phenomenology from first principles. *Journal of High Energy Physics*, 2015(12):1–34, dec 2015.

[3] A.O. Caldeira and A.J. Leggett. Path integral approach to quantum brownian motion. *Physica A: Statistical Mechanics and its Applications*, 121(3):587–616, 1983.

[4] Xiaojian Du, Min He, and Ralf Rapp. In-medium bottomonium production in heavy-ion collisions. *Nuclear Physics A*, 967:904–907, nov 2017.

[5] R.P Feynman and F.L Vernon. The theory of a general quantum system interacting with a linear dissipative system. *Annals of Physics*, 24:118–173, 1963.

[6] Vittorio Gorini, Andrzej Kossakowski, and E. C. G. Sudarshan. Completely positive dynamical semigroups of nâlevel systems. *Journal of Mathematical Physics*, 17(5):821–825, 1976.

[7] R. Katz and P.B. Gossiaux. The schrÃ¶dinger–langevin equation with and without thermal fluctuations. *Annals of Physics*, 368:267–295, may 2016.

[8] Mikko Laine, Owe Philipsen, Marcus Tassler, and Paul Romatschke. Real-time static potential in hot QCD. *Journal of High Energy Physics*, 2007(03):054–054, mar 2007.

[9] G. Lindblad. On the generators of quantum dynamical semigroups. *Communications in Mathematical Physics*, 48(2):119 – 130, 1976.

[10] Oskar Ãlund, Yukinao Akamatsu, Fredrik LaurÃ©n, Takahiro Miura, Jan NordstrÃ¶m, and Alexander Rothkopf. Trace preserving quantum dynamics using a novel reparametrization-neutral summation-by-parts difference operator. *Journal of Computational Physics*, 425:109917, 2021.

[11] Daniel Manzano. A short introduction to the lindblad master equation. *AIP Advances*, 10(2):025106, feb 2020.

[12] Takahiro Miura, Yukinao Akamatsu, Masayuki Asakawa, and Alexander Rothkopf. Quantum brownian motion of a heavy quark pair in the quark-gluon plasma. *Physical Review D*, 101(3), Feb 2020.

[13] J. von Neumann. Wahrscheinlichkeitstheoretischer aufbau der quantenmechanik. *Nachrichten von der Gesellschaft der Wissenschaften zu GÃ¶ttingen, Mathematisch-Physikalische Klasse*, 1927:245–272, 1927.

[14] Alexander Rothkopf. Heavy quarkonium in extreme conditions. *Physics Reports*, 858:1–117, may 2020.

[15] Matthew D. Schwartz. *Quantum field theory and the standard model*. Cambridge University Press, 2014.

[16] Magnus SvÃ€rd and Jan NordstrÃ¶m. Review of summation-by-parts schemes for initialâboundary-value problems. *Journal of Computational Physics*, 268:17–38, 2014.